Estimating the Eddy-Current Modeling Error

Kersten Schmidt[1], Oliver Sterz[2], and Ralf Hiptmair[3]

[1]Seminar for Applied Mathematics, ETH Zurich, CH-8092 Zürich, Switzerland
[2]CST GmbH, 64289 Darmstadt, Germany
[3]Seminar for Applied Mathematics, ETH Zurich, CH-8092 Zürich, Switzerland

The eddy-current model is an approximation of the full Maxwell equations. We will give estimates for the modeling error and show how the constants in the estimates are influenced by the geometry of the problem. Additionally, we analyze the asymptotic behavior of the modeling error when the angular frequency tends to zero. The theoretical results are complemented by numerical examples using high order finite elements. These demonstrate that the estimates are sharp. Hence, this work delivers a mathematical basis for assessing the scope of the eddy-current model.

***Index Terms*—Eddy current model, *hp*-FEM, magnetoquasistatic model, modeling error.**

I. Introduction

In many low-frequency applications the eddy current model is used to describe the electromagnetic fields. The eddy-current model is a *magnetoquasistatic* approximation of the full Maxwell equations (see, e.g., [1]). It is well-known by heuristic arguments that the eddy-current approximation is meaningful if: 1) the diameter D of the computational domain is small compared to the wavelength, $D \ll \lambda$ (quasi-static limit) and 2) and the conductivities are high, $\omega\varepsilon \ll \sigma$, where $\omega > 0$ is the fixed angular frequency, and ε and σ designate the permittivity and the conductivity, respectively.

The modeling error of the eddy-current model has already been considered for instance in [2] and [3]. In this paper, we will present improved estimates as well as an improved asymptotic analysis. Furthermore, we will show that under certain assumptions on the geometry the above conditions are indeed sufficient for a meaningful approximation of the Maxwell equations by the eddy-current model.

The geometric arrangement under consideration is displayed in Fig. 1: we consider the fields in a simple artificially bounded domain $\Omega \subset \mathbb{R}^3, \Omega_C \subset\subset \Omega$ is the union of all conductors where σ is strictly positive, Ω_I is the insulating region where $\sigma \equiv 0$, and $\bar{\Omega} = \bar{\Omega}_C \cup \bar{\Omega}_I$. For simplicity we assume Ω to be contractible.

The *time-harmonic Maxwell equations* read

$$\begin{aligned} \mathbf{curl}\, \boldsymbol{e} &= -i\omega\mu \boldsymbol{h} \\ \mathbf{curl}\, \boldsymbol{h} &= i\omega\varepsilon \boldsymbol{e} + \sigma \boldsymbol{e} + \boldsymbol{j}^0 \end{aligned} \tag{1}$$

with the injected current $\boldsymbol{j}^0 \in L^2(\Omega)$. As usual $\boldsymbol{e}$ and $\boldsymbol{h}$ are the electric and magnetic fields, respectively, and μ is the permeability. In the *time-harmonic eddy-current model* the displacement currents $i\omega\varepsilon\boldsymbol{e}$ are neglected

$$\begin{aligned} \mathbf{curl}\, \boldsymbol{e} &= -i\omega\mu \boldsymbol{h} \\ \mathbf{curl}\, \boldsymbol{h} &= \sigma \boldsymbol{e} + \boldsymbol{j}^0. \end{aligned} \tag{2}$$

Digital Object Identifier 10.1109/TMAG.2008.915834

Color versions of one or more of the figures in this paper are available online at http://ieeexplore.ieee.org.

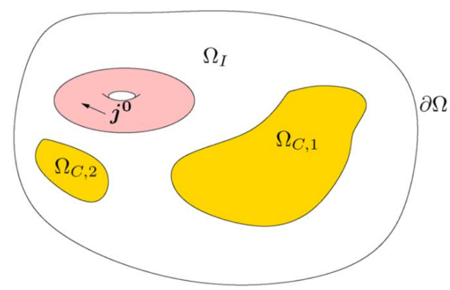

Fig. 1. Geometry, no conductor touches $\partial\Omega$.

Equations (1) and (2) are completed by boundary conditions. Note that in this paper we confine ourselves to perfect magnetic conductor (PMC) boundary conditions on $\partial\Omega$, although our theory covers perfect electric conductor (PEC) boundary conditions or radiation boundary conditions by a Dirichlet-to-Neumann map as well.

The lossy Maxwell equations (1) admit a unique solution $\boldsymbol{e}, \boldsymbol{h} \in H(\mathbf{curl}, \Omega)$ for every $\boldsymbol{j}^0 \in L^2(\Omega)$. For solvability of (2) we assume that $\operatorname{div} \boldsymbol{j}^0 = 0$ in Ω_I, $\int_{\Gamma_k} \boldsymbol{j}^0 \cdot \boldsymbol{n}\, \mathrm{d}S = 0$ for all connected components Γ_k of $\partial\Omega_I \setminus \partial\Omega$ and $\boldsymbol{j}^0 \cdot \boldsymbol{n} = 0$ on $\partial\Omega$. Then, (1) and PMC boundary conditions imply

$$\operatorname{div} \varepsilon \boldsymbol{e} = 0 \text{ in } \Omega_I, \quad \varepsilon \boldsymbol{e} \cdot \boldsymbol{n} = 0 \text{ on } \partial\Omega \tag{3}$$

$$\int_{\Gamma_k} \varepsilon \boldsymbol{e} \cdot \boldsymbol{n}\, \mathrm{d}S = 0 \tag{4}$$

for all connected components $\Gamma_k \setminus \partial\Omega$ of $\partial\Omega_I$. We denote the subspace of $H(\mathbf{curl}, \Omega)$, where (3) and (4) hold, by $\mathcal{X}$. Equations (2) admit a unique solution $\boldsymbol{e} \in \mathcal{X}$ and $\boldsymbol{h} \in H(\mathbf{curl}, \Omega)$, see, e.g., [4].

Now let us call the solution to the Maxwell equations $\boldsymbol{e}^m, \boldsymbol{h}^m$ and define the modeling error fields $\delta\boldsymbol{e} := \boldsymbol{e}^m - \boldsymbol{e}$, $\delta\boldsymbol{h} := \boldsymbol{h}^m - \boldsymbol{h}$. Thus, we arrive at the equations for the modeling error

$$\begin{aligned} \mathbf{curl}\, \delta\boldsymbol{e} &= -i\omega\mu \delta\boldsymbol{h} \\ \mathbf{curl}\, \delta\boldsymbol{h} &= i\omega\varepsilon \boldsymbol{e}^m + \sigma \delta\boldsymbol{e} \end{aligned} \tag{5}$$

which is an eddy-current model with source term $i\omega\varepsilon\boldsymbol{e}^m$.

II. Norms

We denote the L^2 inner product by $(\boldsymbol{a}, \boldsymbol{b})_\Omega := \int_\Omega \boldsymbol{a} \cdot \boldsymbol{b}^* \mathrm{d}x$ and the associated norm by $\| \cdot \|_{L^2(\Omega)}$.

Let us consider the well-known formulas for the dissipation power loss and the magnetic energy

$$P_{\text{Eddy}} = \frac{1}{2}(\sigma \boldsymbol{e}, \boldsymbol{e})_{\Omega_C}$$
$$W_{\text{magn}} = \frac{1}{2}(\mu \boldsymbol{h}, \boldsymbol{h})_{\Omega} = \frac{1}{2\omega^2}\left(\frac{1}{\mu}\mathbf{curl}\,\boldsymbol{e}, \mathbf{curl}\,\boldsymbol{e}\right)_{\Omega}.$$

Combining the two quantities, we define the *power norm*

$$\|\boldsymbol{e}\|^2_{\mathfrak{P},\Omega} := \frac{1}{\omega}\left(\frac{1}{\mu}\mathbf{curl}\,\boldsymbol{e}, \mathbf{curl}\,\boldsymbol{e}\right)_{\Omega} + (\sigma \boldsymbol{e}, \boldsymbol{e})_{\Omega_C}$$

for fields $\boldsymbol{e} \in \mathcal{X}$. This choice justified by the fact, that the magnetic energy is dominant in the Eddy current model.

III. Bounds for the Modeling Error

By (5) estimates for $\delta\boldsymbol{e}$ are linked to stability bounds for the eddy current model. We determine those based on the weak formulation of (5): seek $\delta\boldsymbol{e} \in \mathcal{X}$ such that for all $\boldsymbol{e}' \in \mathcal{X}$

$$\underbrace{\left(\frac{1}{\mu}\mathbf{curl}\,\delta\boldsymbol{e}, \mathbf{curl}\,\boldsymbol{e}'\right)_{\Omega} + i\omega(\sigma\delta\boldsymbol{e}, \boldsymbol{e}')_{\Omega_C}}_{=:a(\delta\boldsymbol{e},\boldsymbol{e}')} = \omega^2(\varepsilon\boldsymbol{e}^m, \boldsymbol{e}')_{\Omega}. \quad (6)$$

We write $E : H^1(\Omega_C) \mapsto H^1(\Omega)$ for the minimal norm extension operator in Sobolev spaces and $\eta > 0$ for its norm, i.e.,

$$\eta = \sup_{w \in H^1(\Omega_C)\setminus\{0\}} \frac{\|Ew\|_{H^1(\Omega)}}{\|w\|_{H^1(\Omega_C)}} \quad (7)$$

with

$$\|w\|^2_{H^1(\Omega)} := \|w\|^2_{L^2(\Omega)} + \|\operatorname{grad} w\|^2_{L^2(\Omega)}. \quad (8)$$

Lemma III.1: There is a constant $C > 0$ only depending on Ω, such that for all $\boldsymbol{u} \in \mathcal{X}$

$$\|\boldsymbol{u}\|^2_{L^2(\Omega)} \le C(1+\eta)^2 D^2 \|\mathbf{curl}\,\boldsymbol{u}\|^2_{L^2(\Omega)} + 2\eta^2\|\boldsymbol{u}\|^2_{L^2(\Omega_C)}.$$

Proof: Start with the $L^2(\Omega)$-orthogonal Helmholtz decomposition of $\boldsymbol{u} \in \mathcal{X}$

$$\boldsymbol{u} = \boldsymbol{u}^0 + \operatorname{grad}\psi, \quad \operatorname{div}\boldsymbol{u}^0 = 0, \quad \psi \in H^1(\Omega). \quad (9)$$

As we have assumed simple topology of Ω, there is $C = C(\Omega) > 0$ such that

$$\|\boldsymbol{u}^0\|_{L^2(\Omega)} \le CD\|\mathbf{curl}\,\boldsymbol{u}\|_{L^2(\Omega)} \quad (10)$$

which implies

$$\|\operatorname{grad}\psi\|_{L^2(\Omega_C)} \le \|\boldsymbol{u}\|_{L^2(\Omega_C)} + CD\|\mathbf{curl}\,\boldsymbol{u}\|_{L^2(\Omega)}. \quad (11)$$

For $\boldsymbol{w} := \boldsymbol{u}^0 + \operatorname{grad} E\psi$ we find $\boldsymbol{w} = \boldsymbol{u}$ in Ω_C and $\mathbf{curl}\,\boldsymbol{w} = \mathbf{curl}\,\boldsymbol{u}$. By the triangle inequality, definition of η, and (11)

$$\|\boldsymbol{w}\|_{L^2(\Omega)} \le \eta\|\boldsymbol{u}\|_{L^2(\Omega_C)} + CD(1+\eta)\|\mathbf{curl}\,\boldsymbol{u}\|_{L^2(\Omega)}.$$

Finally, note that $\boldsymbol{u}$ has minimal $L^2(\Omega)$-norm among all vectorfields with prescribed rotation and fixed values inside Ω_C. ∎

Let us denote by $\varepsilon_{\max}$ and $\mu_{\max}$ the maximal permittivity and permeability, respectively, and by $\sigma_{\min}$ the minimal conductivity in Ω_C. Further, abbreviating $C_1 := C(1+\eta)^2$ and $C_2 := 2\eta^2$, for $\boldsymbol{u} \in \mathcal{X}$ we obtain the straightforward bound

$$\|\boldsymbol{u}\|_{L^2(\Omega)} \le \left(C_1\omega\mu_{\max}D^2 + \frac{C_2}{\sigma_{\min}}\right)\|\boldsymbol{u}\|^2_{\mathfrak{P},\Omega} \quad (12)$$

which involves the coercivity of $a(\cdot,\cdot)$

$$|a(\boldsymbol{u},\boldsymbol{u})| \ge \frac{\omega}{\sqrt{2}}\|\boldsymbol{u}\|^2_{\mathfrak{P},\Omega}$$
$$\ge \frac{1}{\sqrt{2}}\left(C_1\mu_{\max}D^2 + \frac{C_2}{\omega\sigma_{\min}}\right)^{-1}\|\boldsymbol{u}\|^2_{L^2(\Omega)} \quad (13)$$

for all $\boldsymbol{u} \in \mathcal{X}$. On the other hand, from (6) we conclude

$$|a(\delta\boldsymbol{e},\delta\boldsymbol{e})| \le \varepsilon_{\max}\omega^2\|\boldsymbol{e}^m\|_{L^2(\Omega)}\|\delta\boldsymbol{e}\|_{L^2(\Omega)}. \quad (14)$$

Combining (13) with (12) proves the following theorem.

Theorem III.2: The solution $\delta\boldsymbol{e} \in \mathcal{X}$ of (5) satisfies the inequalities

$$\frac{\|\delta\boldsymbol{e}\|_{L^2(\Omega)}}{\|\boldsymbol{e}^m\|_{L^2(\Omega)}} \le \sqrt{2}\left(C_1\varepsilon_{\max}\mu_{\max}\omega^2D^2 + C_2\frac{\omega\varepsilon_{\max}}{\sigma_{\min}}\right)$$
$$\frac{\|\delta\boldsymbol{e}\|_{\mathfrak{P},\Omega}}{\|\boldsymbol{e}^m\|_{\mathfrak{P},\Omega}} \le \sqrt{2}\left(C_1\varepsilon_{\max}\mu_{\max}\omega^2D^2 + C_2\frac{\omega\varepsilon_{\max}}{\sigma_{\min}}\right).$$

Thus, switching to the eddy current model incurs a small modeling error, if

$$C_1\varepsilon_{\max}\mu_{\max}\omega^2D^2 \ll 1 \quad (15)$$
$$C_2\omega\varepsilon_{\max}\sigma_{\min}^{-1} \ll 1. \quad (16)$$

If C_1, C_2 have moderate size, (15) expresses the well-known condition that quasi-static approximation requires the wavelength of electromagnetic waves to be large compared with the size of the region of interest. In addition, (16) means that dielectric relaxation time is negligible on the timescale ω^{-1} of the excitation.

However, C_1, C_2 can be become big, which happens in case $\eta \gg 1$, that is, whenever a function in $H^1(\Omega_C)$ cannot be extended to Ω without a massive increase of its H^1-norm. This will occur, if the extension must feature steep slopes much larger than those inside Ω_C.

Large η will arise, whenever there are narrow gaps between conducting parts, see Fig. 2(a). In this case a function with small local variations inside Ω_C can have significantly different values on both side of the gap, which entails large gradients for any extension into the gap. This is a mathematical confirmation of the intuition that capacitive effects become important in the presence of narrow gaps separating conductors.

The constant η will also soar for slender conducting structures, see Fig. 2(b). Here, a function that varies slowly in length direction and is constant in the across direction will have an extension that is either large in a substantial area around Ω_C or drops to zero rapidly which means large gradients. In either case, its H^1-norm will be big. This matches the intuition that charge accumulation should be a relevant effect in the presence of pointed geometric features.

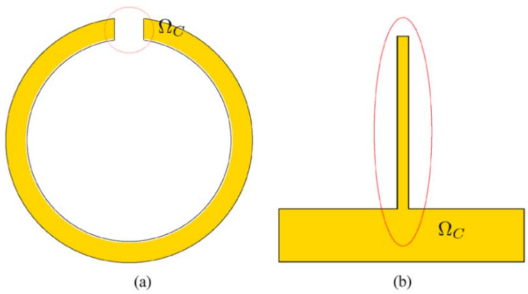

Fig. 2. Geometric situations involving large η. (a) Narrow gap. (b) Thin protrusion.

Note that η from (7), and, hence, C_1 and C_2, can actually be computed for a given geometry by solving the elliptic eigenvalue problem

$$(Eu, Ev)_{H^1(\Omega)} = \eta^2 (u, v)_{H^1(\Omega_C)} \quad \forall v \in H^1(\Omega_C)$$

where $(u, v)_{H^1(\Omega)}$ is the inner product associated with norm (8).

IV. Asymptotic Behavior for $\omega \to 0$

We now consider the asymptotic behavior of the error $\|\delta \boldsymbol{e}\|_{L^2(\Omega)}$ when the angular frequency turns to zero. The key for the asymptotic analysis is a bound for $\|\boldsymbol{e}^m\|_{L^2(\Omega)}$.

Theorem IV.1: Let the material coefficients μ, ε be constant on Ω and σ constant on Ω_C. Let Ω be contractible. Then for the solution $\boldsymbol{e}^m \in \mathcal{X}$ to (1) it holds

$$\|\boldsymbol{e}^m\|_{L^2(\Omega)} \leq \tilde{C}_1 \omega \|\boldsymbol{j}^0\|_{L^2(\Omega)} + \tilde{C}_2 g(\boldsymbol{j}^0)$$

with constants $\tilde{C}_1, \tilde{C}_2$ and

$$g(\boldsymbol{j}^0) := \|\operatorname{div} \boldsymbol{j}^0\|_{L^2(\Omega_C)} + \|[\boldsymbol{j}^0 \cdot \boldsymbol{n}]_{\partial\Omega_C}\|_{L^2(\partial\Omega_C)}$$

where $[\cdot]_{\partial\Omega_C}$ denotes the jump across $\partial\Omega_C$.

Proof: Exploiting that $\boldsymbol{e}^m$ is a solution of a weak formulation of (1) leads to

$$\|\mathbf{curl}\, \boldsymbol{e}^m\|^2_{L^2(\Omega)} \leq \omega\mu \|\boldsymbol{e}^m\|_{L^2(\Omega)} \left(\|\boldsymbol{j}^0\|_{L^2(\Omega)} + \omega\varepsilon \|\boldsymbol{e}^m\|_{L^2(\Omega)} \right).$$

Furthermore, $\|\boldsymbol{e}^m\|_{L^2(\Omega_C)}$ can be bounded by

$$\|\boldsymbol{e}^m\|_{L^2(\Omega_C)} \leq C \left(\frac{1}{|\sigma + i\omega\varepsilon|} \left(g(\boldsymbol{j}^0) + \omega\varepsilon \|\boldsymbol{n} \cdot \boldsymbol{e}^m|_{\Omega_I}\|_{H^{-1/2}(\partial\Omega_C)} \right) + \|\mathbf{curl}\, \boldsymbol{e}^m\|_{L^2(\Omega)} \right). \quad (17)$$

Then, using Lemma III.1, and applying the trace theorem for functions in $H(\operatorname{div}; \Omega_I)$ will complete the proof, see [4] for details. ∎

Note that the assumption on the material coefficients in Theorem IV.1 can be relaxed to a more general case easily.

The function $g(\boldsymbol{j}^0) \geq 0$ represents the amount of direct current injection into the conductor, i.e., it plays the role of a *galvanic connection* between source current and conductor. We see that the asymptotic behavior depends on whether $g(\boldsymbol{j}^0)$ vanishes or not. Both situations are depicted in Fig. 3.

In both cases, we assume that $\boldsymbol{j}^0$ does not depend on ω for small frequencies. Then, by using Theorem III.2, we obtain the following final results for the asymptotic behavior of the modeling error.

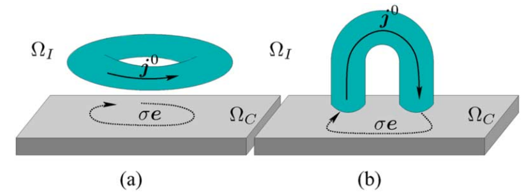

Fig. 3. (a) Without galvanic connection. (b) With galvanic connection.

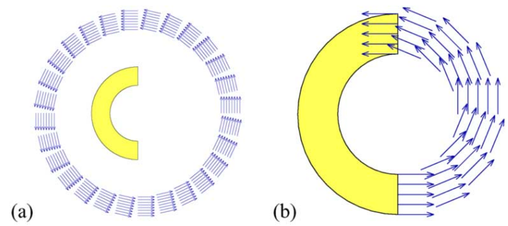

Fig. 4. Geometries of the numerical experiments. (a) No galvanic connection, a circular coil (displayed by arrows) around a conductive half ring. (b) Galvanic connection between injective current and a conductive half ring.

A. Without Galvanic Connection

An ω_0 exists, such that for $0 \leq \omega < \omega_0$ we have $\|\boldsymbol{e}^m\|_{L^2(\Omega)} \leq \tilde{C}\omega \|\boldsymbol{j}^0\|_{L^2(\Omega)}$. The asymptotic modeling error for $\omega \to 0$ reads

$$\|\delta \boldsymbol{e}\|_{L^2(\Omega)} = O(\omega^2).$$

For the power norm we achieve the same result.

B. With Galvanic Connection

For $0 \leq \omega < \omega_0$ we have $\|\boldsymbol{e}^m\|_{L^2(\Omega)} \leq \tilde{C} g(\boldsymbol{j}^0)$. Now we end up with only a linear modeling error for $\omega \to 0$

$$\|\delta \boldsymbol{e}\|_{L^2(\Omega)} = O(\omega).$$

Again, we obtain the same result for the power norm.

V. Numerical Experiments

We investigate the modeling error numerically for the two different cases, in a setting with translational symmetry in one coordinate direction, which allows 2D modeling.

Firstly, we compute the modeling error depending on ω for a circular coil (radii 4.5 m and 5.5 m) that induces eddy currents in a conductive half-ring (radii 1.5 m and 2.5 m, $\sigma = 10^5 (\Omega\,\mathrm{m})^{-1}$) inside a circular domain with radius 7.5 m, see Fig. 4(a). Secondly, we apply an injected current with galvanic connection to the half ring, see Fig. 4(b). In both cases the amount of the injected current is $|\boldsymbol{j}^0| = 1$ A/m^2 and $\varepsilon = 10^{-6}$ As/(Vm).

The computations are based on an $\boldsymbol{h}$-formulation with PMC boundary conditions, discretized with finite elements of high polynomial order (*hp*-FEM) in the software *Concepts* [5]. We observe that the asymptotic estimates are sharp—both with and without galvanic connection (see Fig. 5).

Note that high order discretization is necessary in order to ensure that the discretization error will not dominate the modeling error.

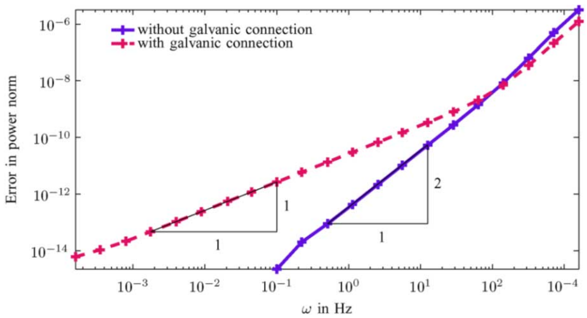

Fig. 5. Error in power norm for a half ring. The solid line is without galvanic connection, the dashed line with galvanic connection.

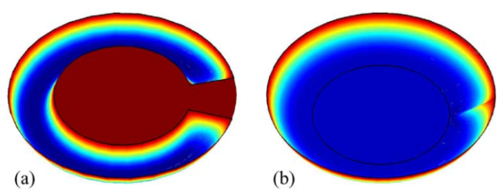

Fig. 6. Amplitude of the magnetic field for a ring with a: (a) wide slit ($d = 1$ m) and (b) very narrow slit ($d = 0.92$ nm).

Next, we consider a conducting cylinder with a slit of width $d > 0$, see Fig. 6. For $d = 0$ the ring is closed. As explained in Section III, this geometry foils eddy current modeling for small d. At $\omega = 2\pi \cdot 50$ Hz we vary d and investigate the impact on the modeling error. The ring geometry of the previous experiment is retained, whereas the coil is now located right at the surface of the conductor.

For a wide slit the exact magnetic field is expected to penetrate into the ring, where it will be almost constant. For a very narrow slit capacitive coupling will allow a current to flow around the ring, which effectively shields the exterior magnetic field. The full Maxwell solutions depicted in Fig. 6 mirror this expected behavior.

Yet capacitive coupling is impossible in the framework of the eddy current model. It will produce a constant magnetic field in the slit and inside the ring regardless of d. Thus, for $d \ll 1$ there will be a large eddy current modeling error, which becomes negligible as d approaches the width of the ring.

Fig. 7 compares Ohmic losses computed based on Maxwell's equations and the eddy current model, respectively. The former is regarded the master model. The number are gleaned from highly accurate hp-FEM computation in each case. For large d and $d \ll 1$ Fig. 7 confirms the above predictions. An interesting transition takes place at $d = 10^{-6}$ m: there ω comes close to the resonant frequency of an LC-circuit comprised of the ring and the slit as capacitor. Thus, the true fields become very large, but the eddy current model will never detect the resonance.

Thus, as plotted in Fig. 8, the eddy current solution will be utterly wrong for d below the critical value d_c of roughly 10^{-6} m. For larger d the modeling error seems to decrease proportional to $(d - d_c)^{-1}$. The solutions are computed on two refinement

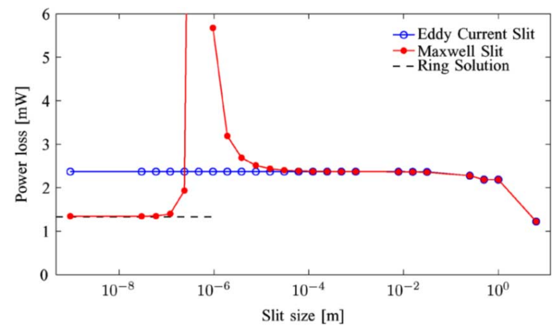

Fig. 7. Ohmic loss for both models for a ring with a slit as a function of slit width.

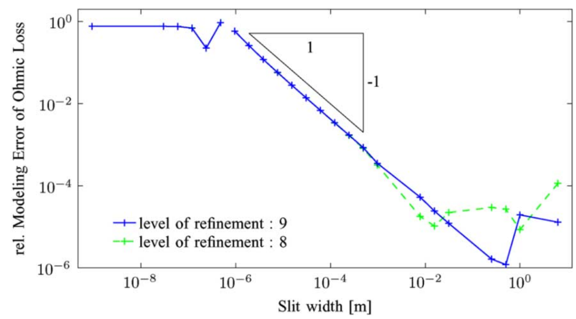

Fig. 8. Relative modeling error of dissipation power loss for a ring with a slit in dependence of slit size for two refinement levels.

levels. Clearly, Fig. 8 also shows that for slit widths less than 10^{-3} m the influence of the discretization error is negligible.

VI. Conclusion

Our results clearly demonstrate scope and limitations of the eddy-current model. By mathematical arguments we have revealed the impact of special geometric situations on the modeling error. Now there is a rigorous mathematical underpinning of the known heuristics guiding the use of the eddy current model.

References

[1] A. Bossavit, *Computational Electromagnetism. Variational Formulation, Complementarity, Edge Elements*, ser. Academic Press Electromagnetism Series. San Diego, CA: Academic Press, 1998, no. 2.

[2] H. Ammari, A. Buffa, and J.-C. Nédélec, "A justification of eddy currents model for the Maxwell equations," *SIAM J. Appl. Math.*, vol. 60, no. 5, pp. 1805–1823, 2000.

[3] A. Alonso, "A mathematical justification of the low-frequency heterogeneous time-harmonic Maxwell equations," *Math. Models Methods Appl. Sci.*, vol. 9, no. 3, pp. 475–489, 1999.

[4] O. Sterz, "Modellierung und Numerik Zeitharmonischer Wirbelstromprobleme in 3D," Ph.D. dissertation, Univ. Heidelberg, Heidelberg, Germany, 2003.

[5] P. Frauenfelder and C. Lage, "Concepts—An object-oriented software package for partial differential equations," *Math. Model. Numer. Anal.*, vol. 36, no. 5, pp. 937–951, Sep. 2002.

Manuscript received June 24, 2007. Corresponding author: K. Schmidt (e-mail: kersten.schmidt@sam.math.ethz).